ACS APPLIED MATERIALS & INTERFACES

Research Article

www.acsami.org

Measurement of Exciton Diffusion in a Well-Defined Donor/Acceptor Heterojunction based on a Conjugated Polymer and Cross-Linked Fullerene Derivative

Yanbin Wang,[†] Hiroaki Benten,*[,†] Shunji Ohara,[†] Daichi Kawamura,[†] Hideo Ohkita,[†,‡] and Shinzaburo Ito*[,†]

[†]Department of Polymer Chemistry, Graduate School of Engineering, Kyoto University, Katsura, Nishikyo, Kyoto 615-8510, Japan

[‡]Japan Science and Technology Agency (JST), PRESTO, 4-1-8 Honcho Kawaguchi, Saitama 332-0012, Japan

Supporting Information

ABSTRACT: We designed a well-defined donor/acceptor heterojunction for measuring exciton diffusion lengths in conjugated polymers. To obtain an insoluble electron acceptor layer, a new cross-linkable fullerene derivative (bis-PCBVB) was synthesized by functionalizing [6,6]-diphenyl-C_{62}-bis(butyric acid methyl ester) (bis-PCBM) with two styryl groups. The spin-coated bis-PCBVB film was cross-linked in situ by heating at 170 °C for 60 min. Surface characterizations by UV−visible absorption, atomic force microscopy, and photoelectron yield spectroscopy revealed that a smooth and solvent-resistant film (*p*-PCBVB) was obtained. In bilayer films with a donor conjugated polymer, poly[2,7-(9,9-didodecylfluorene)-*alt*-5,5-(4′,7′-bis(2-thienyl)-2′,1′,3′-benzothiadiazole)] (PF12TBT), spin-coated on top of the *p*-PCBVB acceptor layer, the photoluminescence (PL) of the PF12TBT was effectively quenched. This is because the highest occupied molecular orbital (HOMO) and lowest unoccupied molecular orbital (LUMO) energy levels of the *p*-PCBVB film are nearly the same as those of the parent bis-PCBM spin-coated film. On the basis of the PL quenching results, the exciton diffusion length and exciton diffusion coefficient in the PF12TBT were evaluated to be 11 nm and 9.8 × 10^{-4} cm^2 s^{-1}, respectively.

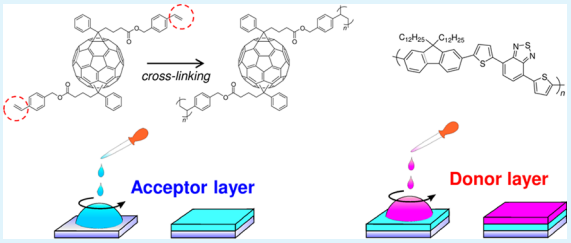

KEYWORDS: *exciton diffusion length, exciton diffusion coefficient, cross-linking, fullerene, conjugated polymer, fluorene-based copolymer, fluorescence quenching, planar heterojunction*

1. INTRODUCTION

Conjugated polymers have great potential for application in organic solar cells because of their efficient light absorption and excellent charge transport properties, combined with simple solution-based processing and inherently low-cost manufacturing.[1,2] The most widely studied polymer-based solar cells have a bulk-heterojunction photovoltaic layer in which an electron donor polymer is mixed with a fullerene-based acceptor.[2,3] For polymer-based organic solar cells, the diffusion of singlet excitons of polymers to the heterojunction is a very important step. The excitons must diffuse from the polymer to the interface with the fullerenes, where they can dissociate to form separated electron and hole states by breaking the strong exciton binding energy.[4−7] However, in most conjugated polymers, singlet excitons can diffuse only a limited distance during their short lifetimes.[8] Therefore, the size of the phase-separated polymer domains in bulk-heterojunction structures should be comparable to the diffusion length of the excitons. Consequently, it is important to measure the exciton diffusion length accurately to guide optimization of both the structure and morphology of the photovoltaic layers.

To date, the exciton diffusion length L_D in conjugated polymers has been evaluated by several methods,[8] including exciton−exciton annihilation,[9−11] the photovoltaic response of solar cells,[12−14] microwave conductivity,[15] and steady-state or time-resolved photoluminescence (PL) quenching measurements.[16−26] Among these, one of the most popular methods is the measurement of steady-state PL quenching on a bilayer system consisting of a conjugated polymer as electron donor and an electron-accepting material. The steady-state PL quenching technique is simple and versatile, as it does not need the high temporal resolution and/or high excitation intensity required for time-resolved PL quenching and exciton−exciton annihilation measurements.[16−18,25,26] In this method, the L_D can be directly evaluated from the dependence of the steady-state PL quenching efficiency on the polymer donor-layer thickness.

For the measurement of steady-state PL quenching in bilayer systems, the donor/acceptor interface forming the planar heterojunction should be flat and smooth, and efficient short-range quenching of excitons via interfacial electron transfer is desirable. Fullerene (C_{60}) and its derivatives such as [6,6]-phenyl-C_{61}-butyric acid methyl ester (PCBM) are suitable for use in electron-accepting quenching layers, because of ultrafast

Received: June 2, 2014
Accepted: July 22, 2014
Published: July 22, 2014

Scheme 1. Synthetic Route for Bis-PCBVB and Chemical Structures of Bis-PCBM, Bis-PCBA, and *p*-PCBVB

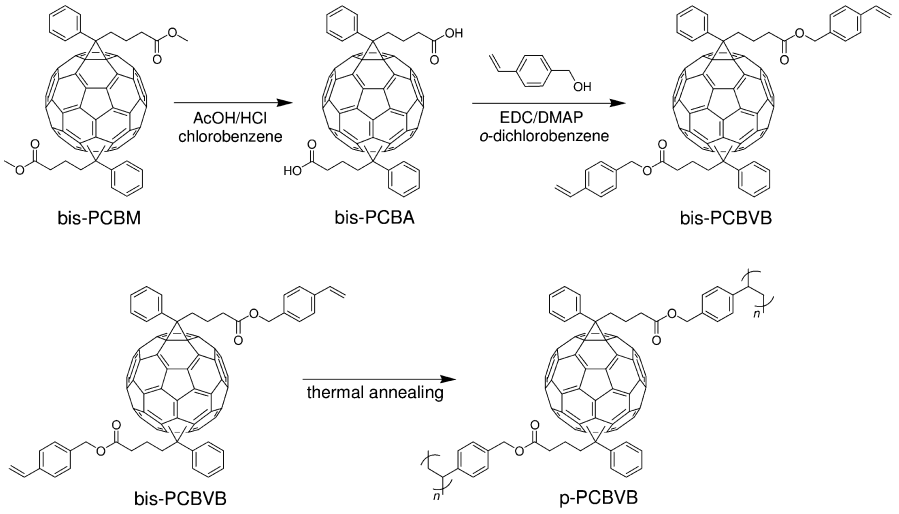

electron transfer at the interface with the conjugated polymers and limited absorption in the visible region.[27−29] Therefore, C_{60} compounds have been employed as the quenching layers in donor/acceptor bilayers to evaluate the L_D of donor polymers. However, recent studies have shown that low-molecular-weight fullerenes are likely to diffuse into the polymer layers even at room temperature, resulting in the loss of the defined donor/acceptor interface.[30−34] Thus, the L_D would be overestimated in such intermixed quasi-bilayer systems.[20]

Such diffusion of small molecules can be effectively suppressed by cross-linking the material. This is also beneficial for designing well-defined multilayer structures because it can impart solvent-resistance to thin films.[35,36] Herein, we synthesized a thermally cross-linkable fullerene derivative by introducing two styryl groups (bis-PCBVB, Scheme 1). The styryl group can be easily polymerized in the solid state even at low temperature.[37−41] With a well-defined bilayer based on the cross-linked bis-PCBVB, the exciton diffusion length and exciton diffusion coefficient of poly[2,7-(9,9-didodecylfluorene)-*alt*-5,5-(4′,7′-bis(2-thienyl)-2′,1′,3′-benzothiadiazole)] (PF12TBT, Figure 1) were evaluated.

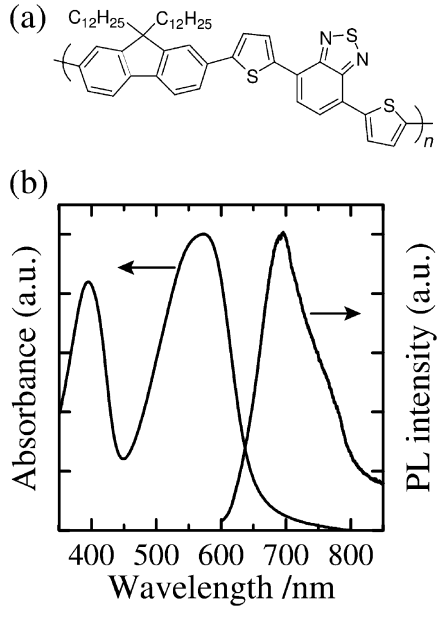

Figure 1. (a) Chemical structure of PF12TBT. (b) Absorption (left) and photoluminescence (right) spectra of a PF12TBT neat film.

2. RESULTS AND DISCUSSION

2.1. Synthesis of Cross-Linkable Fullerene. To design a well-defined polymer/fullerene bilayer heterojunction, the cross-linkable fullerene component should satisfy the following requirements. First, the reactive units should be introduced without changing the electronic structure of the parent fullerene molecules. Second, the cross-linkable fullerene should be sufficiently soluble to form a uniform thin film by spin-coating. Third, the precursor film should be easily polymerized in the solid state and the resulting film should be insoluble in common organic solvents. Finally, the reactive units should be inactive both optically and electronically after the cross-linking. Markov et al. have reported a thermally cross-linkable fullerene bearing carefully designed diacetylene groups; they successfully fabricated a polymer/fullerene bilayer heterojunction by using the insoluble fullerene film.[20] However, not all diacetylenes undergo polymerization in the solid state because they need a favorable stacking alignment for efficient polymerization.[42,43] Moreover, polydiacetylenes have extended π-conjugation throughout the polymer chains,[42,43] and might electronically interact with the fullerene and donor polymers. To avoid these drawbacks, we selected the styryl group as a reactive unit because it is easily synthesized and can be polymerized in the solid state even at low temperature.[37−41] Furthermore, the polystyrene structure formed by the cross-linking of styryl groups is inactive both optically and electronically. We also selected [6,6]-phenyl-C_{62}-bis(butyric acid methyl ester), bis-PCBM,[44] as a parent fullerene molecule, because two cross-linkable units can be introduced without changing the core electronic structure of bis-PCBM, as will be discussed below.

As shown in Scheme 1, a thermally cross-linkable fullerene bearing two styryl groups (bis-PCBVB) was synthesized. Hydrolysis of bis-PCBM gave the corresponding diacid, bis-PCBA.[45,46] 4-Vinylbenzyl alcohol was synthesized according to the literature method.[47] The bis-styryl ester, bis-PCBVB, was synthesized by the esterification of bis-PCBA with 4-vinylbenzyl alcohol in the presence of EDC and DMAP. In the FT-IR spectra of the compounds, as shown in Figure 2a, the carbonyl stretching vibration was shifted from 1737 to 1706 cm^{-1} after the hydrolysis of bis-PCBM, indicating formation of bis-PCBA

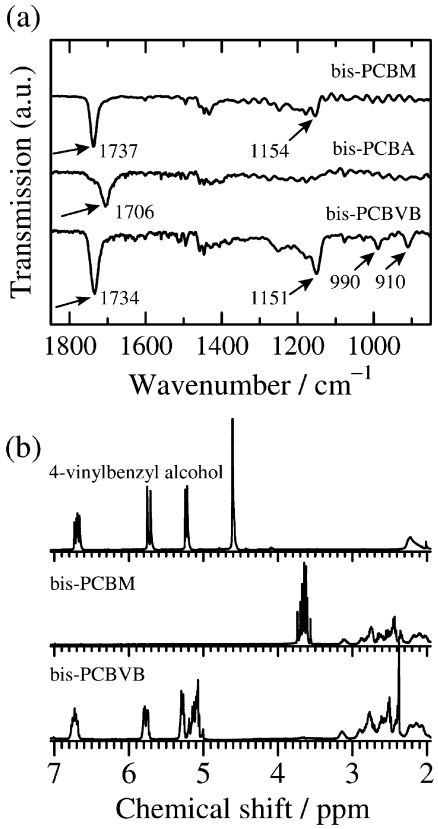

Figure 2. (a) FT-IR spectra of bis-PCBM, bis-PCBA, and bis-PCBVB. (b) ^{1}H NMR spectra of 4-vinylbenzyl alcohol, bis-PCBM, and bis-PCBVB.

by the ester-to-acid conversion. The carbonyl stretching vibration returned to 1734 cm^{-1} and vibrational stretches due to the vinyl groups appeared at 910 and 990 cm^{-1} after the esterification of bis-PCBA. Although the stretching band of the C−O bond of the ester group disappeared in the bis-PCBA spectrum, it was observed at 1154 cm^{-1} in bis-PCBM and 1151 cm^{-1} in bis-PCBVB. Moreover, as shown in Figure 2b, the ^{1}H NMR spectra of the two esters revealed that the methyl group signal at 3.69 ppm in bis-PCBM was absent in the bis-PCBVB spectrum, and was replaced by signals of the styryl groups at 6.73−6.66, 5.78−5.70, and 5.28−5.25 ppm. These changes in the FT-IR and ^{1}H NMR spectra support the successful modification of bis-PCBM to bis-PCBVB.

2.2. Cross-Linking of Fullerene. To thermally cross-link the styryl groups, we spin-coated a bis-PCBVB film from chlorobenzene solution onto a glass substrate and then heated under nitrogen atmosphere at selected temperatures for various lengths of time. The solvent resistance of the resulting cross-linked films (*p*-PCBVB) was studied by UV−visible absorption spectroscopy. When the bis-PCBVB film was heated at 170 °C for 60 min, no absorption change was observed before and after spin-rinsing with chlorobenzene, indicating both the full cross-linking of the bis-PCBVB monomers and the film's insolubility (Figure 3). The annealing temperature of 170 °C is reasonably close to the temperature required for the thermal cross-linking reaction of styryl units.[40,41,48] The film resulting from the thermal polymerization of a fullerene with a single styryl group exhibited a reduction in absorbance by approximately 26% after washing with chlorobenzene.[48] With a single styryl substituent, linear fullerene polymers may be predominantly formed, which

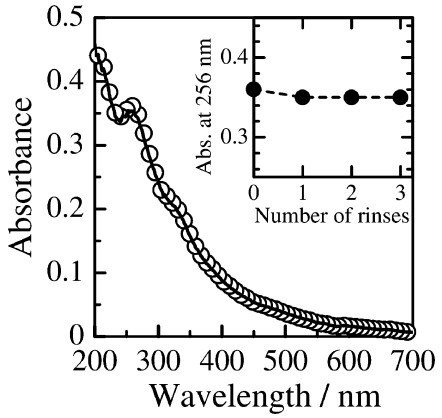

Figure 3. Absorption spectra of bis-PCBVB film annealed at 170 °C for 60 min (circles) and after rinsing with chlorobenzene (solid line). The inset shows the absorbance at 256 nm of the annealed bis-PCBVB film measured after spin-rinsing with chlorobenzene several times.

would not provide the needed solvent resistance.[49] On the other hand, the bis-PCBVB monomer bearing two styryl groups can form cross-linked networks, which provide superior solvent resistance. Figure 4 shows topographical and phase images of

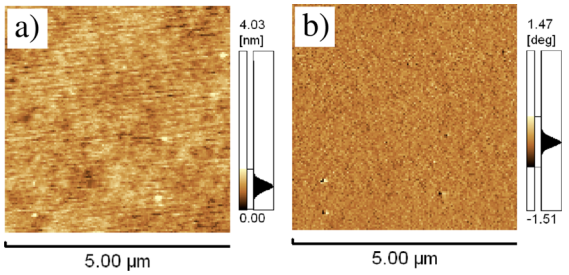

Figure 4. AFM tapping mode (a) height and (b) phase images of bis-PCBVB thin film after thermal annealing at 170 °C for 60 min and then spin-rinsing with chlorobenzene (5 μm × 5 μm).

the *p*-PCBVB film after spin-rinsing with chlorobenzene: the surface is smooth and uniform with a root-mean-square roughness of 0.81 nm. The atomic force microscopy (AFM) images demonstrate that the surface of the *p*-PCBVB layer is not eroded by the subsequent spin-coating of a conjugated polymer layer from chlorobenzene solution. We further examined the wetting properties of the *p*-PCBVB surface in comparison to that of the bis-PCBM surface. From the contact angle measurement,[50,51] the surface energy was evaluated to be 30.0 mJ m^{-2} for the *p*-PCBVB film, which was almost the same as that of the bis-PCBM spin-coated film (30.6 mJ m^{-2}). In summary, the in situ cross-linked bis-PCBVB films are solvent resistant and exhibit a pinhole-free and smooth surface with a surface energy similar to that of bis-PCBM.

2.3. Optical and Electrical Properties. Figure 5a shows the absorption spectra of bis-PCBM (circles) and bis-PCBVB (solid line) measured in THF solution. Both fullerene derivatives exhibit essentially the same spectrum with the same molar absorption coefficients ε, indicating that the electronic structure of the core fullerene in bis-PCBVB is the same as that of the parent bis-PCBM even after the styryl group functionalization. To confirm the electron-accepting ability of bis-PCBVB, the energy level of the lowest unoccupied molecular orbital (LUMO) was evaluated by cyclic voltammetry in solution. The LUMO energy level of bis-PCBVB was

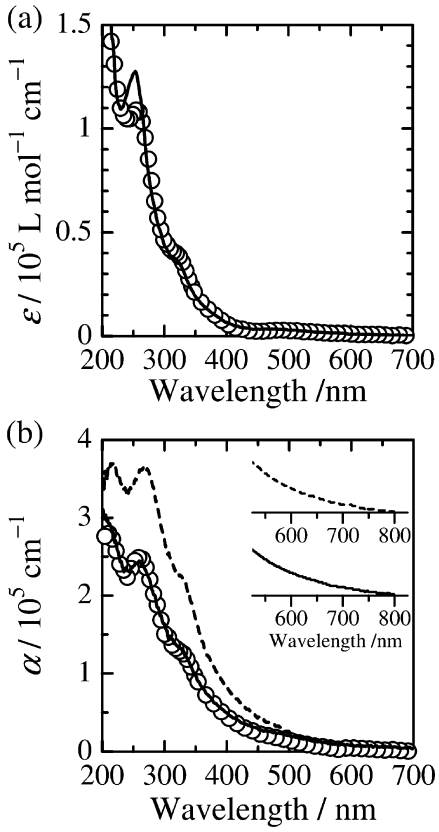

Figure 5. (a) Molar absorption coefficients ε of bis-PCBM (circles) and bis-PCBVB (solid line) measured in THF. (b) Absorption coefficients α of bis-PCBM (broken line), bis-PCBVB (circles), and *p*-PCBVB (solid line) films. The inset shows the absorption of bis-PCBM (broken line) and *p*-PCBVB (solid line) films at longer wavelength.

−3.64 eV, which is the same as that of bis-PCBM measured under the same experimental conditions (see the Supporting Information). We note that the LUMO energy level is very similar to that of previously reported bis-PCBM (−3.61 eV).[52] In addition, the PL quenching was also examined for a conjugated polymer film blended with bis-PCBVB. Here, we selected the fluorene-based copolymer, PF12TBT, since fluorene-based copolymers are some of the most popular conjugated polymers used for efficient polymer-based solar cells.[53] The PL quenching efficiencies were 8 and 33% for the PF12TBT films blended with 0.1 and 1 wt % bis-PCBVB, respectively. The PL from PF12TBT was quenched completely (quenching efficiency of ∼100%) in the film blended with 50 wt % bis-PCBVB. These values of PL quenching efficiencies are the same as those for the PF12TBT films blended with bis-PCBM. The deep LUMO energy level and efficient PL quenching, equivalent to those of bis-PCBM, ensures that bis-PCBVB acts as an effective electron acceptor.

We next investigated the optical and electrical properties of the fullerene films. Figure 5b shows the absorption coefficients α of thin films of bis-PCBM (broken line), bis-PCBVB (circles), and *p*-PCBVB (solid line) spin-coated on quartz substrates. The α value for the *p*-PCBVB film was the same as that of bis-PCBVB, indicating that the electronic structure of the core fullerene in bis-PCBVB is not altered by the cross-linking reactions of the styryl groups. On the other hand, the α value of the *p*-PCBVB film was smaller than that of the bis-PCBM film. The reduction in α is attributable to an increase in the molecular volume due to the introduction of the two cross-linkable units, which would decrease the density of the C_{60} core units in the bis-PCBVB film as compared with that of bis-PCBM.

The electron-accepting ability of the *p*-PCBVB film in terms of energetics was next examined. The highest occupied molecular orbital (HOMO) energy level of the *p*-PCBVB was evaluated to be −6.0 eV by photoelectron yield spectroscopy. The LUMO energy level was roughly estimated to be −4.3 ∼ −4.5 eV by adding the onset energy of the optical absorption (750−800 nm, shown in the inset in Figure 5b) to the HOMO energy. The HOMO and LUMO energy levels of the *p*-PCBVB film agreed well with those of the bis-PCBM film determined in the same manner. The deep LUMO energy level of the *p*-PCBVB film, equivalent to that of the bis-PCBM film, reveals that the *p*-PCBVB surface can act as an electron acceptor for typical conjugated polymer donors.

2.4. Thermal Stability of D/A Bilayer Structure. To investigate the thermal stability of the bilayer structure, we measured the PL intensity of a PF12TBT/*p*-PCBVB bilayer sample before and after the sample was heated at 140 °C for 60 min in a N_2 atmosphere. Note that the annealing temperature (140 °C) is far above the glass transition temperature T_g of PF12TBT (T_g = 81 °C). Figure 6 shows the PL spectra of a

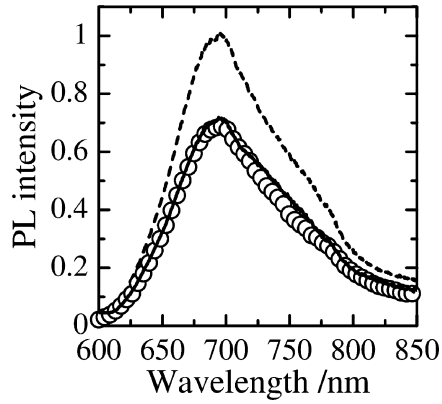

Figure 6. PL spectra of 30 nm thick PF12TBT film spin-coated on quartz substrate (broken line), and on *p*-PCBVB surfaces before (circles) and after thermal annealing at 140 °C for 60 min (solid line). The PL intensities were normalized by the PL intensity of the PF12TBT film spin-coated on the quartz substrate.

PF12TBT/*p*-PCBVB bilayer film before (circles) and after (solid line) heating, together with that of a PF12TBT reference film without a *p*-PCBVB layer (broken line). No change in the PL intensity was observed for either bilayer sample before and after heating: the PL intensity was quenched by the *p*-PCBVB layer to 70% relative to that of the reference film. If the thermal annealing induced interlayer mixing of *p*-PCBVB with PF12TBT and hence eroded the flat interfacial structure, the PL intensity would decrease because of an increase in the donor/acceptor interface available for exciton dissociation.[20] However, this is not the case, as shown in the figure. The same PL intensities before and after heating indicate the absence of intermixing between the PF12TBT and *p*-PCBVB layers under these experimental conditions. This stability is in contrast to previous studies reported for bilayer samples prepared by evaporating fullerene onto a polymer film[20,30,33] or by laminating a polymer layer onto a fullerene spin-coated

film.[31,34] The thermal stability of the *p*-PCBVB film is beneficial for designing a well-defined donor/acceptor bilayer in which to precisely evaluate the exciton diffusion length.

2.5. Exciton Diffusion in PF12TBT Film. Finally, we discuss the exciton diffusion in PF12TBT on the basis of the PL quenching efficiency in the PF12TBT/*p*-PCBVB bilayer samples. The thickness of the PF12TBT layer L was systematically varied from 14 to 71 nm, whereas that of the *p*-PCBVB layer was fixed at 20 nm. For comparison, PF12TBT neat films with the same thicknesses as the PF12TBT in the bilayers were also prepared. For both bilayer and reference samples, PF12TBT was selectively excited at 580 nm from the side of the PF12TBT/air interface. Figure 7a shows the PL spectra of the bilayer samples. In this figure, the PL intensities of the bilayer samples $I(L)$ are normalized by those of the corresponding PF12TBT reference films $I_0(L)$. The relative PL intensity $I(L)/I_0(L)$ decreases with the decreasing thickness of the PF12TBT, meaning that a larger portion of PF12TBT excitons reaches the interface with the *p*-PCBVB acceptor in the thinner PF12TBT.

To evaluate the exciton diffusion length, we analyzed the PL quenching data on the basis of a one-dimensional diffusion model.[20,22] Here, we assume an infinite exciton quenching rate at the PF12TBT/*p*-PCBVB interface and no exciton quenching at the PF12TBT/air interface. The interference of the excitation light inside the polymer film is neglected, and an exponential attenuation of the light intensity, given by $\propto \exp(-\alpha L)$, was assumed as an initial exciton distribution in the PF12TBT layer.[20,22] Under these assumptions, the steady-state exciton quenching efficiency $Q(L)$ is given by eq 1[20,22]

$$Q(L) = 1 - \frac{I(L)}{I_0(L)} = \frac{[\alpha^2 L_D^2 + \alpha L_D \tanh(L/L_D)]\exp(-\alpha L) - \alpha^2 L_D^2 [\cosh(L/L_D)]^{-1}}{(1 - \alpha^2 L_D^2)[1 - \exp(-\alpha L)]} \quad (1)$$

where α is the absorption coefficient at the excitation wavelength and L_D is the exciton diffusion length in the direction normal to the acceptor surface (Figure 7c). In this model, we assume one-dimensional exciton diffusion, and the exciton diffusion length L_D is defined as $L_D = \sqrt{D\tau_0}$.[20,22] As shown in Figure 7b, the best-fitting curve by eq 1 is obtained for an exciton diffusion length of 11 nm (solid line). The L_D and the diffusion coefficient D have been reported mostly within the range of 5–8 nm and $(3–30) \times 10^{-4}$ cm^2 s^{-1}, respectively, for amorphous conjugated polymers such as poly(*p*-phenylenevinylene) (PPV) and its derivatives.[11,17,21,22,54] The diffusion length of 11 nm estimated for PF12TBT is slightly larger than that reported previously.

To address the origin of the larger L_D in PF12TBT, we evaluated D of a PF12TBT singlet exciton. Figure 8 shows the PL decay curve of a PF12TBT neat film obtained by time-correlated single photon counting (TCSPC) measurements. The PL decay was well-fitted by a single exponential function with a lifetime of τ_0 = 1.24 ns. Consequently, the diffusion coefficient was evaluated to be $D = 9.8 \times 10^{-4}$ cm^2 s^{-1} from the relationship $L_D = \sqrt{D\tau_0}$, with L_D = 11 nm and τ_0 = 1.24 ns. The diffusion constant is well consistent with those reported for various amorphous conjugated polymers ($(3–30) \times 10^{-4}$ cm^2 s^{-1}) as mentioned above.[11,17,21,22,54] On the other hand, the exciton lifetime of PF12TBT is relatively longer: most conjugated polymers such as PPV derivatives exhibit PL lifetimes shorter than 1 ns.[19,22,23] Thus, the large L_D in the PF12TBT is attributed to the relatively long singlet exciton lifetime of 1.24 ns. This is probably because the PF12TBT excitons do not suffer from structural- and chemical-defect-related nonradiative quenching in the film.[18,19,22] In addition, the Förster radius was calculated as 2.0 nm for PF12TBT to *p*-PCBVB (see the Supporting Information).[55] Therefore, we note that the energy transfer is also contributable to an increase in the L_D value.

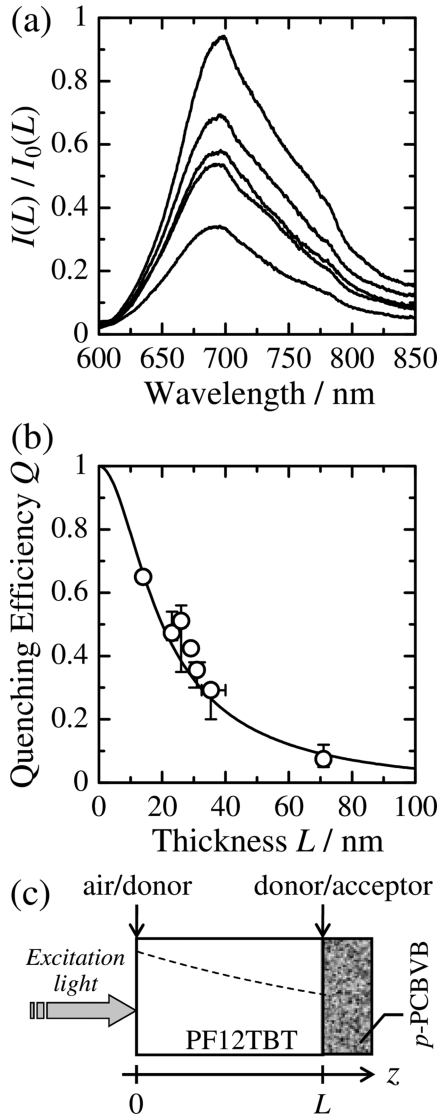

Figure 7. (a) PL intensity $I(L)$ of PF12TBT/*p*-PCBVB bilayer films with different PF12TBT thicknesses. The intensity of each bilayer film is normalized against the intensity $I_0(L)$ of a PF12TBT reference film with the corresponding thickness. (b) PL quenching efficiencies $Q(L)$ of PF12TBT/*p*-PCBVB bilayer films with different PF12TBT thicknesses: experimental (circles) and calculated (solid line) values. The calculations were performed using eq 1 with an L_D of 11 nm. (c) Schematic of the bilayer structure used in the PL quenching measurements. The choice of coordinate z used in eq 1 is shown. PF12TBT was excited at 580 nm from the side of the PF12TBT/air interface. The broken line represents an exponential decay of excitation light inside the polymer film.

3. CONCLUSIONS

A thermally cross-linkable fullerene derivative was designed and synthesized. In situ cross-linking was carried out by annealing

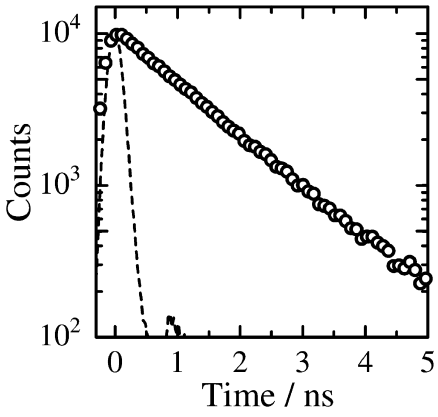

Figure 8. PL decay curve of a PF12TBT neat film spin-coated on a quartz substrate. The excitation and monitoring wavelengths were 640 and 700 nm, respectively. The broken line shows an instrumental response function.

the bis-PCBVB thin film at 170 °C for 60 min, giving a solvent-resistant and thermally stable film with a flat and smooth surface. The LUMO energy level of the film, equivalent to that of the parent fullerene, indicates that the film can act as a good electron-accepting layer. On the basis of the PL quenching in the bilayer films, the exciton diffusion length and diffusion coefficient of PF12TBT were determined as L_D = 11 nm and D = 9.8 × 10^{-4} cm^2 s^{-1}, respectively. Our donor/acceptor bilayer system is widely applicable to systematic studies of L_D in various conjugated polymers.

4. EXPERIMENTAL SECTION

4.1. Materials. The starting reactants [6,6]-diphenyl-C_{62}-bis-(butyric acid methyl ester) (bis-PCBM) and 4-vinylbenzyl chloride were purchased from Aldrich Chemical Co. 4-(Dimethylamino)-pyridine (DMAP) and 1-ethyl-3-(3-(dimethylamino)propyl)-carbodiimide (EDC) were purchased from Tokyo Chemical Industry Co., Ltd., and Wako Pure Chemical Industries Ltd., respectively. The PF12TBT was synthesized and characterized at Sumitomo Chemical Co., Ltd. The weight-average molecular weight M_w, polydispersity index (PDI, given by M_w/M_n, where M_n is the number-average molecular weight), and glass transition temperature T_g were 26,900 g mol^{-1}, 3.4, and 81 °C, respectively. Other reagents and solvents were purchased from Nacalai Tesque and Wako Pure Chemical Industries Ltd., respectively, and used as received without any further purification.

4.2. General Measurement and Characterization. ^{1}H NMR spectra were recorded on a JEOL JNM-AL400 (400 MHz) in deuterated chloroform. FTIR spectra were recorded with a Jasco FT/IR-4200 spectrophotometer using the KBr pellet method for thin film study. Absorption spectra were measured with a Hitachi U-3500 spectrophotometer.

The cyclic voltammetry measurements were performed using a potentiostat/galvanostat (Princeton Applied Research, model 273A) in an Ar-bubbled *o*-dichlorobenzene/acetonitrile (4:1 (v/v)) solution containing 0.1 M of tetrabutylammonium perchlorate as a supporting electrolyte with an Ag/Ag^+ (0.01 M $AgNO_3$) as a reference electrode, a Pt wire as a counter electrode, and Pt as a working electrode with an area of 2.0 mm^2. The scan rate was set to 250 mV s^{-1}.

The steady-state PL spectra were measured with a calibrated fluorescence spectrophotometer (Hitachi, F-4500) equipped with a photomultiplier (Hamamatsu, R928F). The PL quenching efficiency of PF12TBT films blended with bis-PCBM and bis-PCBVB was evaluated from the ratio of the PL intensity of PF12TBT for the blended film to that for a PF12TBT neat film (after each PL intensity was corrected for variations in the PF12TBT absorption at 580 nm). Excitation of the blend and neat films was performed at 580 nm. For both PF12TBT/*p*-PCBVB bilayer and PF12TBT neat films, PF12TBT was selectively excited at 580 nm from the side of the PF12TBT/air interface. The PL quenching efficiency of PF12TBT in the bilayer films was evaluated from the ratio of the PL intensity for the PF12TBT/*p*-PCBVB bilayer film to that for a PF12TBT neat film. The PL decay curve was measured by the TCSPC technique with a photon counting system (HORIBA Jobin Yvon, FluoroCube), and the decay curve was analyzed with DAS6 decay analysis software (HORIBA). The PF12TBT film was excited at 640 nm with a pulsed laser diode (HORIBA Jobin Yvon, NanoLED-635L) and the emission was collected at 700 nm. The total instrument response function has a full-width at half-maximum (fwhm) of ca. 260 ps for the PL decay measurement. The steady-state PL spectra and PL decay measurements were obtained under a N_2 atmosphere.

The AFM surface images were collected in tapping mode (Shimadzu, SPM-9600) using silicon probes (Nanoworld, NCHR) with a tip radius typically smaller than 8 nm. The film thickness was evaluated by contact-mode measurement as follows: a part of the film was scratched out with a sharp needle to expose the substrate, and the film thickness was evaluated from the height difference between the film and substrate surfaces.

The HOMO energy levels of the bis-PCBM and *p*-PCBVB neat films were estimated by photoelectron yield spectroscopy (Riken Keiki, AC-3).

The surface energies γ_X of the materials were examined by contact angle θ_X measurements on spin-coated films of material X using both water and ethylene glycol at room temperature, and were then evaluated by the harmonic mean method.[50,51]

4.3. Synthesis of 4-Vinylbenzyl Acetate. A mixture of 4-vinylbenzyl chloride (10 mL, 0.071 mol) and potassium acetate (8 g, 0.0815 mol) in DMSO (30 mL) was stirred at 40 °C for 2 days under N_2 atmosphere. The reaction mixture was poured into water and extracted three times with ethyl acetate. The collected ethyl acetate layers were dried with anhydrous $MgSO_4$. After removal of the solvent, the residue was purified by column chromatography on silica gel with ethyl acetate/hexane (1:10, v/v) as eluent to afford the product (11.96 g, 96%) as a yellow oil. ^{1}H NMR (400 MHz, $CDCl_3$, δ): 2.09 (s, 3H), 5.08 (s, 2H), 5.24 (d, J = 10.8 Hz, 1H), 5.73 (d, J = 17.6 Hz, 1H), 6.67 (dd, J = 11.2, 11.2 Hz, 1H), 7.30 (d, J = 12 Hz, 2H), 7.39 (d, J = 8 Hz, 2H).

4.4. Synthesis of 4-Vinylbenzyl Alcohol. Sodium hydroxide (2.45 g, 0.061 mol) was added to a solution of 4-vinylbenzyl acetate (3.60 g, 0.024 mol) in ethanol (10 mL) and water (3 mL) under a N_2 atmosphere. After stirring at room temperature for 20 min, the reaction mixture was heated to 80 °C slowly and stirred for a further 2 h. It was then poured into water, extracted three times with ethyl acetate, and then dried with anhydrous $MgSO_4$. After removal of the solvent, the residue was purified by column chromatography on silica gel with ethyl acetate/hexane (1:5, v/v) as eluent to afford the product (2.66 g, 96%) as a dark brown oil. ^{1}H NMR (400 MHz, $CDCl_3$, δ): 2.22 (s, 1H), 4.61 (s, 2H), 5.21 (d, J = 11.2 Hz, 1H), 5.71 (d, J = 17.6 Hz, 1H), 6.66 (dd, J = 10.8, 10.8 Hz, 1H), 7.26 (d, J = 8.0 Hz, 2H), 7.36 (d, J = 8.0 Hz, 2H).

4.5. Synthesis of Bis-[6,6]-phenyl-C_{62}-butyric Acid (bis-PCBA). To a solution of bis-PCBM (0.1 g, 0.09 mmol) in chlorobenzene (40 mL) was added acetic acid (12 mL) and concentrated hydrochloric acid (8 mL). The mixture was stirred and refluxed overnight. The course of the reaction was monitored by TLC (ethyl acetate/hexane (1:10, v/v)), which showed an R_f change after complete conversion from 0.95 to 0.68. The solvent was removed in vacuo and the precipitate was collected by filtration. The crude product was washed with methanol and hexane several times to afford bis-PCBA (0.082 g, 81.2%) as a dark brown powder. FTIR (KBr pellet, cm^{-1}) ν: 1702, 1430, 1424, 1204, 1179, 1150, 719, 566, 525.

4.6. Synthesis of Bis-[6,6]-phenyl-C_{62}-butyric Acid vinylbenzyl Ester (bis-PCBVB). 4-Vinylbenzyl alcohol (50 mg, 0.373 mmol) was mixed with bis-PCBA (81.5 mg, 0.074 mmol) and DMAP (27.4 mg, 0.224 mmol) in *o*-dichlorobenzene (20 mL). The mixture was stirred for 1 h and then cooled to 0 °C in an ice/water bath. Finally, EDC (60 mg, 0.33 mmol) was added to the mixture quickly via

syringe. The mixture was stirred at 0 °C for 5 h and then warmed to room temperature with continuous stirring for 12 h. After removal of the solvent under reduced pressure, the residue was purified by silica gel chromatography using chloroform/methanol (20:1, v/v) as eluent to afford the product (61.7 mg, 62.6%) as a dark brown solid. ^{1}H NMR (400 MHz, $CDCl_3$, δ) 2.05−3.12 (m, 12H), 5.13−5.03 (m, 4H), 5.28−5.25 (m, 2H), 5.78−5.70 (m, 2H), 6.73−6.66 (m, 2H), 7.93−7.31 (m, 18H). FTIR (KBr pellet, cm^{-1}) ν: 1734, 1627, 1602, 1495, 1426, 1249, 1177, 1149, 910, 713, 572, 526.

■ ASSOCIATED CONTENT

Supporting Information

Cyclic voltammograms, calculation of Förster radius for PF12TBT to *p*-PCBVB, dependence of PL intensity on the absorption of the PF12TBT neat film. This material is available free of charge via the Internet at http://pubs.acs.org

■ AUTHOR INFORMATION

Corresponding Authors

*E-mail: benten@photo.polym.kyoto-u.ac.jp. Tel.: +81 75 383 2614. Fax: +81 75 383 2617.

*E-mail: sito@photo.polym.kyoto-u.ac.jp. Tel.: +81 75 383 2612. Fax: +81 75 383 2617.

Notes

The authors declare no competing financial interest.

■ ACKNOWLEDGMENTS

This work was supported by the CREST program from the Japan Science and Technology Agency (JST), the Iketani Science and Technology Foundation, and the Japan Society for the Promotion of Science (JSPS) through the "Funding Program for World-Leading Innovative R&D on Science and Technology (FIRST Program)," initiated by the Council for Science and Technology Policy (CSTP). Further support was obtained through a Grant-in-Aid for Young Scientists (B) (22750109) from the JSPS. Y. Wang is sponsored by the China Scholarship Council (CSC).

■ REFERENCES

(1) Søndergaard, R.; Hösel, M.; Angmo, D.; Larsen-Olsen, T. T.; Krebs, F. C. Roll-to-Roll Fabrication of Polymer Solar Cells. *Mater. Today* **2012**, *15*, 36−49.

(2) Li, G.; Zhu, R.; Yang, Y. Polymer Solar Cells. *Nat. Photonics.* **2012**, *6*, 153−161.

(3) Brabec, C. J.; Gowrisanker, S.; Halls, J. J. M.; Laird, D.; Jia, S.; Williams, S. P. Polymer-Fullerene Bulk-Heterojunction Solar Cells. *Adv. Mater.* **2010**, *22*, 3839−3856.

(4) Gregg, B. A. The Photoconversion Mechanism of Excitonic Solar Cells. *MRS Bull.* **2005**, *30*, 20−22.

(5) Deibel, C.; Dyakonov, V. Polymer-Fullerene Bulk Heterojunction Solar Cells. *Rep. Prog. Phys.* **2010**, *73*, 096401.

(6) Ohkita, H.; Ito, S. Transient Absorption Spectroscopy of Polymer-Based Thin-Film Solar Cells. *Polymer* **2011**, *52*, 4397−4417.

(7) Peumans, P.; Yakimov, A.; Forrest, S. R. Small Molecular Weight Organic Thin-Film Photodetectors and Solar Cells. *J. Appl. Phys.* **2003**, *93*, 3693−3723.

(8) Menke, S. M.; Holmes, R. J. Exciton Diffusion in Organic Photovoltaic Cells. *Energy Environ. Sci.* **2014**, *7*, 499−512.

(9) Tamai, Y.; Matsuura, Y.; Ohkita, H.; Benten, H.; Ito, S. One-Dimensional Singlet Exciton Diffusion in Poly(3-hexylthiophene) Crystalline Domains. *J. Phys. Chem. Lett.* **2014**, *5*, 399−403.

(10) Cook, S.; Liyuan, H.; Furube, A.; Katoh, R. Singlet Annihilation in Films of Regioregular Poly(3-hexylthiophene): Estimates for Singlet Diffusion Lengths and the Correlation between Singlet Annihilation Rates and Spectral Relaxation. *J. Phys. Chem. C* **2010**, *114*, 10962−10968.

(11) Lewis, A. J.; Ruseckas, A.; Gaudin, O. P. M.; Webster, G. R.; Burn, P. L.; Samuel, I. D. W. Singlet Exciton Diffusion in MEH-PPV Films Studied by Exciton-Exciton Annihilation. *Org. Electron.* **2006**, *7*, 452−456.

(12) Huijser, A.; Savenije, T. J.; Shalav, A.; Siebbeles, L. D. A. An Experimental Study on the Molecular Organization and Exciton Diffusion in a Bilayer of a Porphyrin and Poly(3-hexylthiophene). *J. Appl. Phys.* **2008**, *104*, 034505.

(13) Pettersson, L. A. A.; Roman, L. S.; Inganäs, O. Modeling Photocurrent Action Spectra of Photovoltaic Devices Based on Organic Thin Films. *J. Appl. Phys.* **1999**, *86*, 487−496.

(14) Halls, J. J. M.; Pichler, K.; Friend, R. H.; Moratti, S. C.; Holmes, A. B. Exciton Diffusion and Dissociation in a Poly(*p*-phenylenevinylene)/C_{60} Heterojunction Photovoltaic Cell. *Appl. Phys. Lett.* **1996**, *68*, 3120−3122.

(15) Kroeze, J. E.; Savenije, T. J.; Vermeulen, M. J. W.; Warman, J. M. Contactless Determination of the Photoconductivity Action Spectrum, Exciton Diffusion Length, and Charge Separation Efficiency in Polythiophene-Sensitized TiO_2 Bilayers. *J. Phys. Chem. B* **2003**, *107*, 7696−7705.

(16) Leow, C.; Ohnishi, T.; Matsumura, M. Diffusion Lengths of Excitons in Polymers in Relation to External Quantum Efficiency of the Photocurrent of Solar Cells. *J. Phys. Chem. C* **2014**, *118*, 71−76.

(17) Scully, S. R.; McGehee, M. D. Effects of Optical Interference and Energy Transfer on Exciton Diffusion Length Measurements in Organic Semiconductors. *J. Appl. Phys.* **2006**, *100*, 034907.

(18) Theander, M.; Yartsev, A.; Zigmantas, D.; Sundström, V.; Mammo, W.; Andersson, M. R.; Inganäs, O. Photoluminescence Quenching at a Polythiophene/C_{60} Heterojunction. *Phys. Rev. B* **2000**, *61*, 12957−12963.

(19) Haugeneder, A.; Neges, M.; Kallinger, C.; Spirkl, W.; Lemmer, U.; Feldmann, J.; Scherf, U.; Harth, E.; Gügel, A.; Müllen, K. Exciton Diffusion and Dissociation in Conjugated Polymer/Fullerene Blends and Heterostructures. *Phys. Rev. B* **1999**, *59*, 15346−15351.

(20) Markov, D. E.; Amsterdam, E.; Blom, P. W. M.; Sieval, A. B.; Hummelen, J. C. Accurate Measurement of the Exciton Diffusion Length in a Conjugated Polymer Using a Heterostructure with a Side-Chain Cross-Linked Fullerene Layer. *J. Phys. Chem. A* **2005**, *109*, 5266−5274.

(21) Mikhnenko, O. V.; Azimi, H.; Scharber, M.; Morana, M.; Blom, P. W. M.; Loi, M. A. Exciton Diffusion Length in Narrow Bandgap Polymers. *Energy Environ. Sci.* **2012**, *5*, 6960−6965.

(22) Markov, D. E.; Tanase, C.; Blom, P. W. M.; Wildeman, J. Simultaneous Enhancement of Charge Transport and Exciton Diffusion in Poly(*p*-phenylene vinylene) Derivatives. *Phys. Rev. B* **2005**, *72*, 045217.

(23) Markov, D. E.; Hummelen, J. C.; Blom, P. W. M.; Sieval, A. B. Dynamics of Exciton Diffusion in Poly(*p*-phenylene vinylene)/Fullerene Heterostructures. *Phys. Rev. B* **2005**, *72*, 045216.

(24) Shaw, P. E.; Ruseckas, A.; Samuel, I. D. W. Exciton Diffusion Measurements in Poly(3-hexylthiophene). *Adv. Mater.* **2008**, *20*, 3516−3520.

(25) Fushimi, T.; Oda, A.; Ohkita, H.; Ito, S. Triplet Energy Migration in Layer-by-Layer Deposited Ultrathin Polymer Films Bearing Tris(2,2′-bipyridine)ruthenium(II) Moieties. *J. Phys. Chem. B* **2004**, *108*, 18897−18902.

(26) Masuda, K.; Ikeda, Y.; Ogawa, M.; Benten, H.; Ohkita, H.; Ito, S. Exciton Generation and Diffusion in Multilayered Organic Solar Cells Designed by Layer-by-Layer Assembly of Poly(*p*-phenylenevinylene). *ACS Appl. Mater. Interfaces* **2010**, *2*, 236−245.

(27) Brabec, C. J.; Zerza, G.; Cerullo, G.; Silvestri, S. D.; Luzzati, S.; Hummelen, J. C.; Sariciftci, S. Tracing Photoinduced Electron Transfer Process in Conjugated Polymer/Fullerene Bulk Heterojunctions in Real Time. *Chem. Phys. Lett.* **2001**, *340*, 232−236.

(28) Guo, J.; Ohkita, H.; Benten, H.; Ito, S. Charge Generation and Recombination Dynamics in Poly(3-hexylthiophene)/Fullerene Blend Films with Different Regioregularities and Morphologies. *J. Am. Chem. Soc.* **2010**, *132*, 6154−6164.

(29) Yamamoto, S.; Ohkita, H.; Benten, H.; Ito, S.; Yamamoto, S.; Kitazawa, D.; Tsukamoto, J. Efficient Charge Generation and Collection in Amorphous Polymer-Based Solar Cells. *J. Phys. Chem. C* **2013**, *117*, 11514−11521.
(30) Schlebusch, C.; Kessler, B.; Cramm, S.; Eberhardt, W. Organic Photoconductors and C_{60}. *Synth. Met.* **1996**, *77*, 151−154.
(31) Treat, N. D.; Brady, M. A.; Smith, G.; Toney, M. F.; Kramer, E. J.; Hawker, C. J.; Chabinyc, M. L. Interdiffusion of PCBM and P3HT Reveals Miscibility in a Photovoltaically Active Blend. *Adv. Energy Mater.* **2011**, *1*, 82−89.
(32) Rochester, C. W.; Mauger, S. A.; Moulé, A. J. Investigating the Morphology of Polymer/Fullerene Layers Coated Using Orthogonal Solvents. *J. Phys. Chem. C* **2012**, *116*, 7287−7292.
(33) Stevens, D. M.; Qin, Y.; Hillmyer, M. A.; Frisbie, C. D. Enhancement of the Morphology and Open Circuit Voltage in Bilayer Polymer/Fullerene Solar Cells. *J. Phys. Chem. C* **2009**, *113*, 11408−11415.
(34) Collins, B. A.; Gann, E.; Guignard, L.; He, X.; McNeill, C. R.; Ade, H. Molecular Miscibility of Polymer-Fullerene Blends. *J. Phys. Chem. Lett.* **2010**, *1*, 3160−3166.
(35) Zuniga, C. A.; Barlow, S.; Marder, S. R. Approaches to Solution-Processed Multilayer Organic Light-Emitting Diodes Based on Cross-Linking. *Chem. Mater.* **2011**, *23*, 658−681.
(36) Huang, F.; Cheng, Y. J.; Zhang, Y.; Liu, M. S.; Jen, A. K. -Y. Crosslinkable Hole-Transporting Materials for Solution Processed Polymer Light-Emitting Diodes. *J. Mater. Chem.* **2008**, *18*, 4495−4509.
(37) Khuong, K. S.; Jones, W. H.; Pryor, W. A.; Houk, K. N. The Mechanism of the Self-Initiated Thermal Polymerization of Styrene. Theoretical Solution of a Classic Problem. *J. Am. Chem. Soc.* **2005**, *127*, 1265−1277.
(38) Chong, Y. K.; Rizzardo, E.; Solomon, D. H. Confirmation of the Mayo Mechanism for the Initiation of the Thermal Polymerization of Styrene. *J. Am. Chem. Soc.* **1983**, *105*, 7761−7762.
(39) Mayo, F. R. The Dimerization of Styrene. *J. Am. Chem. Soc.* **1968**, *90*, 1289−1295.
(40) Sun, H.; Liu, Z.; Hu, Y.; Wang, L.; Ma, D.; Jing, X.; Wang, F. Crosslinkable Poly(*p*-phenylenevinylene) Derivative. *J. Polym. Sci., Part A: Polym. Chem.* **2004**, *42*, 2124−2129.
(41) Klärner, G.; Lee, J. I.; Lee, V. Y.; Chan, E.; Chen, J. P.; Nelson, A.; Markiewicz, D.; Siemens, R.; Scott, J. C.; Miller, R. D. Cross-Linkable Polymers Based on Dialkylfluorenes. *Chem. Mater.* **1999**, *11*, 1800−1805.
(42) Enkelmann, V. Polydiacetylenes. In *Adv. Polym. Sci.*; Cantow, H. J., Ed.; Springer-Verlag: Berlin, 1984; Vol. *63*, pp 91−136.
(43) Ogawa, T. Diacetylenes in Polymeric Systems. *Prog. Polym. Sci.* **1995**, *20*, 943−985.
(44) Lenes, M.; Wetzelaer, G. J. A. H.; Kooistra, F. B.; Veenstra, S. C.; Hummelen, J. C.; Blom, P. W. M. Fullerene Bisadducts for Enhanced Open-Circuit Voltages and Efficiencies in Polymer Solar Cells. *Adv. Mater.* **2008**, *20*, 2116−2119.
(45) Hummelen, J. C.; Knight, B. W.; LePeq, F.; Wudl, F.; Yao, J.; Wilkins, C. L. Preparation and Characterization of Fulleroid and Methanofullerene Derivatives. *J. Org. Chem.* **1995**, *60*, 532−538.
(46) Hsieh, C. H.; Cheng, Y. J.; Li, P. J.; Chen, C. H.; Dubosc, M.; Liang, R. M.; Hsu, C. S. Highly Efficient and Stable Inverted Polymer Solar Cells Integrated with a Cross-Linked Fullerene Material as an Interlayer. *J. Am. Chem. Soc.* **2010**, *132*, 4887−4893.
(47) Feng, S.; Wang, Q.; Gao, Y.; Huang, Y.; Qing, F. L. Synthesis and Characterization of a Novel Amphiphilic Copolymer Capable as Anti-Biofouling Coating Material. *J. Appl. Polym. Sci.* **2009**, *114*, 2071−2078.
(48) Cho, N.; Yip, H. L.; Hau, S. K.; Chen, K. S.; Kim, T. W.; Davies, J. A.; Zeigler, D. F.; Jen, A. K. -Y. n-Doping of Thermally Polymerizable Fullerenes as an Electron Transporting Layer for Inverted Polymer Solar Cells. *J. Mater. Chem.* **2011**, *21*, 6956−6961.
(49) Cheng, Y. J.; Liu, M. S.; Zhang, Y.; Niu, Y.; Huang, F.; Ka, J. W.; Yip, H. L.; Tian, Y.; Jen, A. K. -Y. Thermally Cross-Linkable Hole-Transporting Materials on Conducting Polymer: Synthesis, Characterization, and Applications for Polymer Light-Emitting Devices. *Chem. Mater.* **2008**, *20*, 413−422.
(50) Wu, S. Calculation of Interfacial Tension in Polymer Systems. *J. Polym. Sci., Part C: Polym. Symp.* **1971**, *34*, 19−30.
(51) Shimizu, R. N.; Demarquette, N. R. Evaluation of Surface Energy of Solid Polymers Using Different Models. *J. Appl. Polym. Sci.* **2000**, *76*, 1831−1845.
(52) Faist, M. A.; Keivanidis, P. E.; Foster, S.; Wöbkenberg, P. H.; Anthopoulos, T. D.; Bradley, D. D. C.; Durrant, J. R.; Nelson, J. Effect of Multiple Adduct Fullerenes on Charge Generation and Transport in Photovoltaic Blends with Poly(3-hexylthiophene-2,5-diyl). *J. Polym. Sci., Part B: Polym. Phys.* **2011**, *49*, 45−51.
(53) Inganäs, O.; Zhang, F.; Andersson, M. R. Alternating Polyfluorenes Collect Solar Light in Polymer Photovoltaics. *Acc. Chem. Res.* **2009**, *42*, 1731−1739.
(54) Mikhnenko, O. V.; Cordella, F.; Sieval, A. B.; Hummelen, J. C.; Blom, P. W. M.; Loi, M. A. Temperature Dependence of Exciton Diffusion in Conjugated Polymers. *J. Phys. Chem. B* **2008**, *112*, 11601−11604.
(55) Förster, T. Transfer Mechanisms of Electronic Excitation. *Discuss. Faraday Soc.* **1959**, *27*, 7−17.